Article

Enhancement of Electrochemical Stability Window and Electrical Properties of CNT-Based PVA−PEG Polymer Blend Composites

Mohd Sadiq, M. Ajmal Khan, Mohammad Moeen Hasan Raza, Shah Masheerul Aalam, Mohammad Zulfequar, and Javid Ali*

Read Online

ACCESS | Metrics & More | Article Recommendations

ABSTRACT: New polymer blend composite electrolytes (PBCEs) were prepared by the solution casting technique using poly(vinyl alcohol) (PVA)-polyethylene glycol (PEG), sodium nitrate ($NaNO_3$) as a doping salt and multiwalled carbon nanotubes (MWCNTs) as fillers. The X-ray diffraction pattern confirms the structural properties of the polymer blend composite films. FTIR investigations were carried out to understand the chemical properties and their band assignments. The ionic conductivity of the 10 wt % MWCNTs incorporated PVA-PEG polymer blend was measured as 4.32×10^{-6} S cm^{-1} at 20 °C and increased to 2.253×10^{-4} S/cm at 100 °C. The dependence of its conductivity on temperature suggests Arrhenius behavior. The equivalent circuit models that represent the $R_s(Q_1(R_1(Q_2(R_2(CR_3)))))$ were used to interpret EIS data. The dielectric behavior of the samples was investigated by utilizing their AC conductance spectra, dielectric permittivity, dielectric constant (ε^i and ε^r), electric modulus (M^i and M^r), and loss tangent tan δ. The dielectric permittivity of the samples increases due to electrode polarization effects in low frequency region. The loss tangent's maxima shift with increasing temperature; hence, the peak height rises in the high frequency region. MWCNTs-based polymer blend composite electrolytes show an enhanced electrochemical stability window (4.0 V), better transference number (0.968), and improved ionic conductivity for use in energy storage device applications.
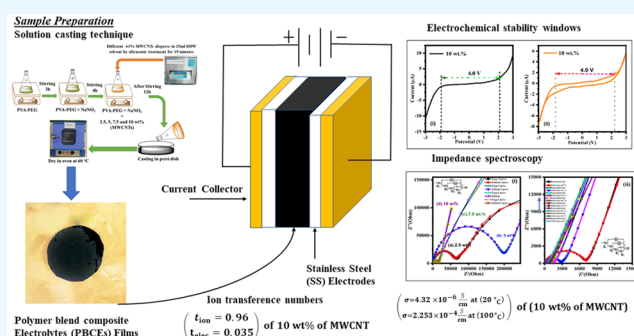
1. INTRODUCTION

In recent times, renewable energy sources have emerged as a viable alternative to meet the expanding demand for clean energy. It may help us to deal with climate change related issues as well as alternative energy resources.[1,2] The electrolyte is a critical component in the operation of several energy storage devices. It functions as a channel for ions to travel between the electrodes through an electrolyte. It behaves as an insulator when the device is completely discharged and stops working properly.[3] Due to the use of liquid in electrolytes, it develops a number of key issues such as flammability, mechanical instability, leakage, and corrosion of metals in devices. Generally, a polymer composite electrolyte is prepared by dissolving inorganic salt in a polymer matrix of having a high molecular weight along with nanofillers.[4] It works as a host medium for ion transport. The mechanism of ion conduction/transportation in solid polymer electrolytes differs from liquid-based electrolytes. The dissociated ions in liquid electrolytes can freely move around.[5,6] While in solid polymer electrolytes, ions move predominantly due to segmental motion of polymer chains and concomitant ion hopping within the polymeric matrix.[7] As a result, polar functional groups on the backbone of a chain are in high demand for conduction mechanism. Furthermore, proper-

ties such as strong mechanical and thermal stability, a wide electrochemical window, compatibility, nontoxicity, and process ability are also important considerations for the above-mentioned purpose. The commercial use of the polymer composite electrolyte requires both low cost and high efficiency.[8,9] Poly(vinyl alcohol) (PVA) has a semicrystalline nature. It has certain properties such as being water-soluble, nontoxic, and environmentally friendly. This biocompatible and biodegradable polymer is converted from polyvinyl acetate. PVA has a high dielectric strength, good thermal and mechanical stability, good charge storage capacity, and environmental stability. Due to these properties, PVA is a widely studied material and extensively used as the polymer membrane for technology applications.[10,11] Similarly, polyethylene glycol (PEG) is another synthetic polymer which has various advantages like, good film formation, low cost, water-soluble,
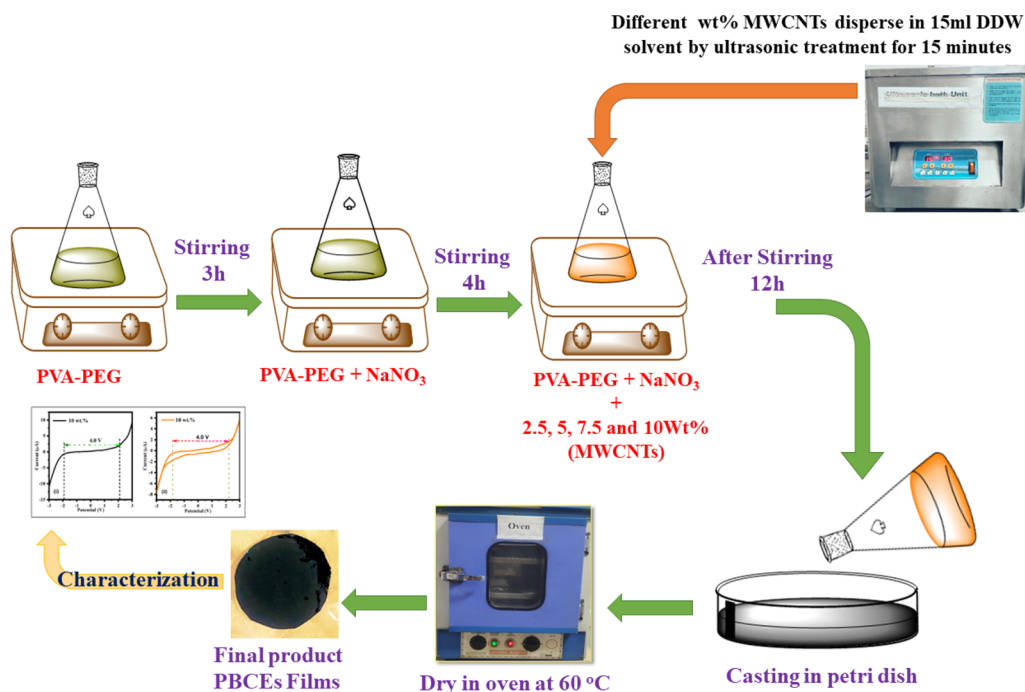
Figure 1. Flowchart of sample preparation by solution cast technique.

compatibilty with the other polymer, and a wide molecular weight range. Polyethylene glycols are known for their ability to retain moisture. Low molecular weight PEGs are hygroscopic. Hence, they are favored for a variety of applications due to their moisture retention properties.[12−14] PEG have a low volatility which gives them the thermal stability needed for a variety of applications. The combination of PVA-PEG network polymers has become one of the most popular materials for scientific studies. In the first network, PEG does more than just contribute to the recovery and self-healing phenomena.[15−17] By mixing the host matrix materials such as polymers with fillers like MWCNT we can achieve the properties of polymer composites with more desirable goals. In recent works on carbon nanotube (CNT) based polymer electrolytes, it is found that the carbon nanotubes are made up of thin cylinders of carbon. The shapes are based on the cylindrical concentric planes on the layer wall. It may be a single layer, double layer, or multilayer structure.[18] CNT-based composite materials have a unique structural property that improves its mechanical, electrical, thermal, and optical properties.[19] Several studies focusing on composites based on poly(vinyl alcohol) (PVA) loaded with carbon nanotubes have been found in the literature. The few examples of the polymer composite are listed as poly(vinyl alcohol) (PVA)+CNT,[20] poly(vinyl alcohol) (PVA)+CNT,[21] poly(vinyl alcohol) (PVA)+MWCNT,[22] poly(vinyl alcohol) (PVA)+CNT,[23] and poly(vinyl alcohol) (PVA)/chitosan/CNT.[24] The majority of research has been focused on functional films. PVA possesses a carbon backbone with hydroxyl groups that can help as a foundation of hydrogen-bonding interactions between the nanofiller to allow blended polymer-based nanocomposites.[25] To achieve the full CNT amplification which contains good interfacial electron affinity with the matrix, a good dispersion in matrix is needed.[26] An improvement in ion transfer properties in the CNT-based polymer matrices is observed. Also, CNT have excellent properties for use as a reinforcing material to improve polymer performance.[27] This new class of fillers is expected to further improve ionic conductivity, reduce crystallinity, and

provide high mechanical properties.[28] Poly(vinyl alcohol) is one of the most researched polymers. They have high mechanical properties, plasticity, and chemical stability. Functionalized CNT/PVA nanocomposite membranes can be used to separate an ethanol/water mixture.[29,30] Furthermore, poly(vinyl alcohol) as the main chain has shown excellent properties under external force. It allows the formation of composites for a variety of applications such as supercapacitors, batteries, and chemical sensors.[31−34]

In the present work, we propose to develop a polymer blend composite electrolytes based on (PVA-PEG) + NaNO$_3$ + x wt % with multiwalled carbon nanotubes (MWCNTs) as fillers which will be prepared through the standard solution cast method. Investigation will be carried out to understand the effect of MWCNTs concentration on the performance of structural, thermal, and ionic conductivity properties. Fourier transform infrared and Raman studies will be performed to understand the chemical bond and structural properties. In addition to the above, we are also interested in understanding the effect of ion dissociation and association with the polymer host matrix by adding MWCNTs. The prepared sample will be checked for conductivity, dielectric characteristics, and an improvement in electrochemical performance. The above key parameters are significant for different applications and can be used in Na-batteries, Li-batteries, and EDLC applications.

2. EXPERIMENTAL DETAILS

2.1. Materials Used. We used poly(vinyl alcohol) (PVA) polymer with a molecular weight of 125000 g/mol and polyethylene glycol (PEG) with a molecular weight of 6000−7500 g/mol (CDH (P) Ltd. India). Sodium nitrate (NaNO$_3$) salts were purchased from Avantor Performance Materials (RAMKEM) India Ltd., purity/assay: 99.0%, and pristine multiwalled carbon nanotubes (MWCNTs) of diameter 30 nm and length few microns as filler were used.

2.2. Preparation of Polymer Blend Composite Electrolytes. Polymer blends (PVA-PEG) containing sodium nitrate
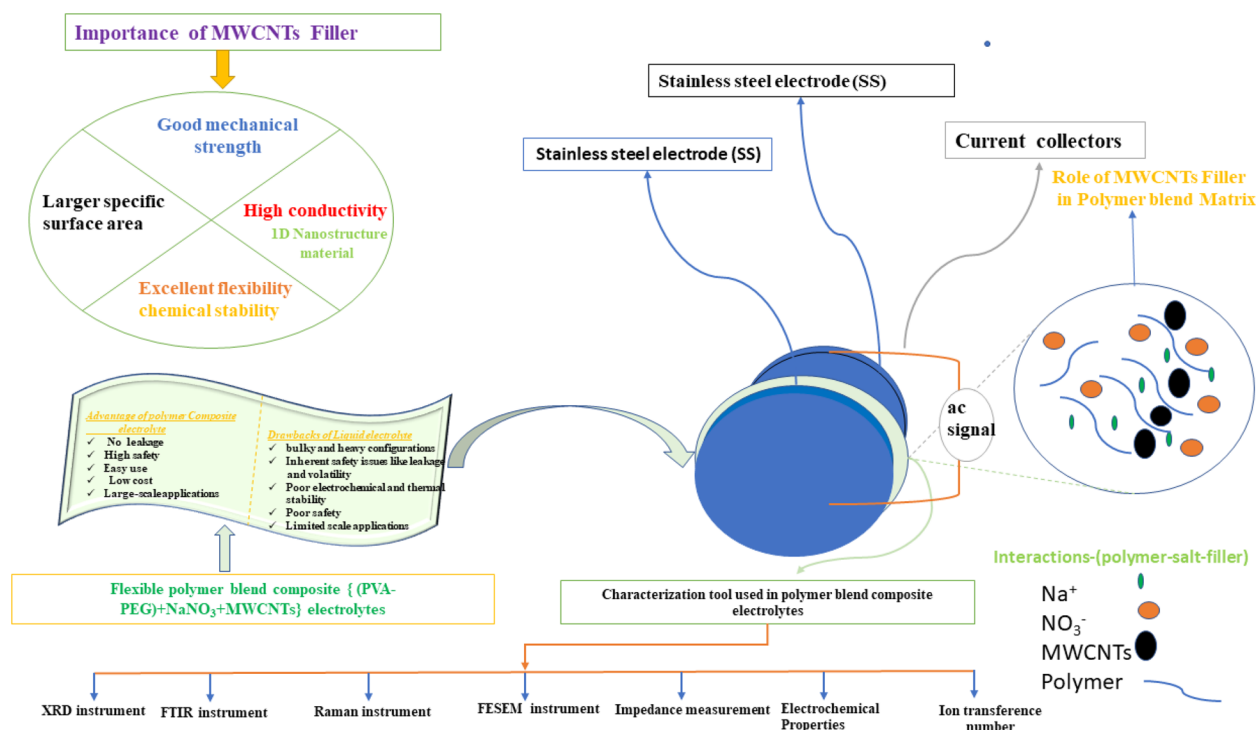
Figure 2. Schematic illustration of interaction process along with sample characterization technique method.
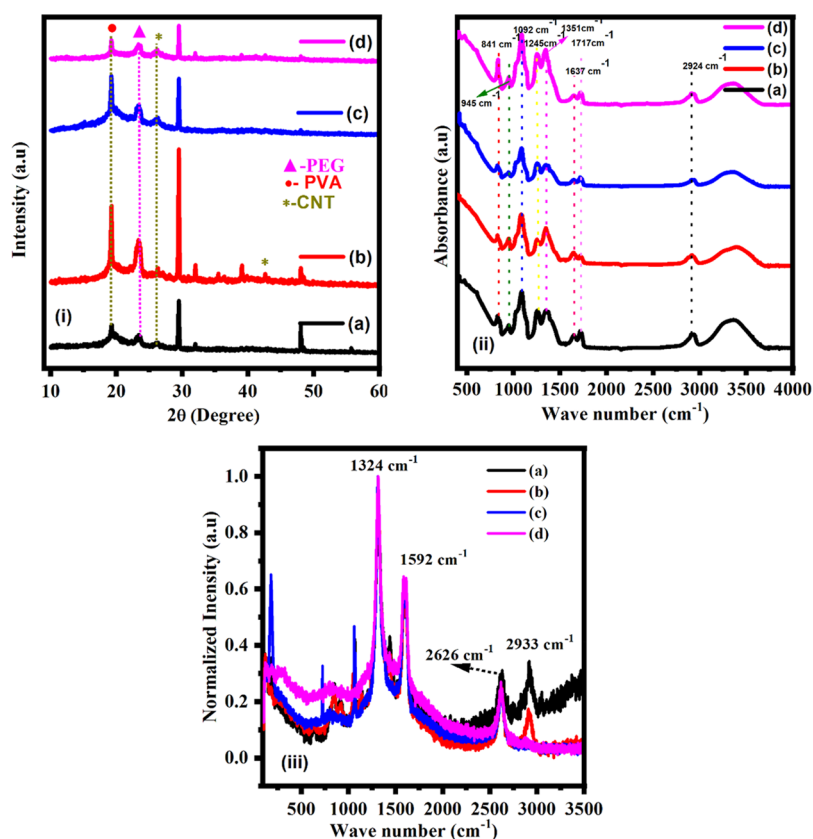
Figure 3. (i) XRD patterns for various contents: (a) 2.5 wt %, (b) 5 wt %, (c) 7.5 wt %, and (d) 10 wt % of MWCNTs fillers. (ii) FT-IR spectra for various contents: (a) 2.5 wt %, (b) 5 wt %, (c) 7.5 wt %, and (d) 10 wt % of MWCNTs fillers. (iii) Raman spectra for various contents: (a) 2.5 wt %, (b) 5 wt %, (c) 7.5 wt %, and (d) 10 wt % of MWCNTs fillers.

($NaNO_3$) and MWCNTs fillers of various weight percent (x = 2.5, 5, 7.5, and 10 wt %) were prepared by standard solution casting techniques.[35] Initially, we added distilled water to PVA

(0.6 g) and PEG (0.4 g) and then put it on a magnetic stirrer for 3 h to get a uniform solution. Again, the blend PVA-PEG solution is mixed with an optimized salt concentration and kept

under magnetic stirring for the next 4 h. The MWCNTs were dispersed separately in the DI water through the 15 min ultrasonicated process. The optimized sodium salt concentration was added to the different wt % of MWCNTs fillers (x wt % = 2.5,5,7.5 and 10 wt %) and stirred for the12 h to get a polymer blend composite solution. The solution was drop cast on Petri dishes and dried in an oven at 60 °C for 2 days until dry. Subsequently, the prepared thin films were peeled from the Petri dishes. The flowchart of the sample preparation is presented in Figure 1.

2.3. Characterization. We have studied the structural properties of the prepared films by XRD equipment with a scan rate of 8° per minute over a range of 10°−60°. Fourier-transform infrared spectroscopy (FTIR) was done to confirmation of the stretching mode and bending mode behavior in the prepared films. The FTIR spectroscopy (Model: Thermo Scientific, NICOLET iS50, -FTIR) has been performed over a wavenumber range of 400−4000 cm^{-1} with a spectral resolution of 4 cm^{-1}. The morphology of the prepared films was obtained by a field emission scanning electron microscope (FESEM) (Zeiss, SIGMA). Raman spectroscopy was performed using an excitation laser of wavelength 785 nm and the signal recorded in the range of 200−3500 cm^{-1} (Model: Renishaw inVia Raman microscope). DSC was performed for a (Model: LABSYS Evo DTA/DSC - 131, France) heating rate of 10 °C/min. The AC-impedance along with dielectric behavior of the prepared films were characterized by a dielectric spectroscopy/impedance analyzer (Alpha A, Novocontrole, Germany) in the frequency range of 10^{-1}−10^7 Hz and temperature range of 20−100 °C.The electrochemical behavior of the films obtained by the two different techniques (1) linear sweep voltammetry (LSV) and (2) cyclic voltammetry (CV) using a potentiostat/galvanostat and impedance analyzer PALMSENS (Netherlands), Model PalmSens4. The ion transference number measurement was done using a chronoamperometry (CA) technique. The interaction process of the films along with the sample characterization technique method are shown in Figure 2.

3. RESULTS AND DISCUSSION

3.1. Analysis of X-ray Diffraction (XRD). The X-ray diffraction spectra of the polymer blend composite electrolytes were characterized in the range of 10−60 (in degree) as shown in Figure 3i(a−d). The obtained peaks are observed at 2θ (in deg) = 19.20, 23.24, 26.30, 29.53, 39.09, 42.68, and 48.13, which confirms the presence of PVA, PEG polymer, NaNO$_3$ salt, and MWCNTs as fillers. The diffraction peak at 19.20° represents a dual amorphous−semicrystalline nature of PVA. The diffraction peaks at 26.30° and 42.68°, 55°in the planes (002) and (100) represents the presence of MWCNTs in the sample.[36,37] The main peaks of pure PEG are observed at 19.20, 23.24, and 26.30 (in °) indicating the crystalline form of PEG.[38,39] The diffraction peaks confirm the crystalline nature of PVA-PEG blends. The intensities of all crystalline peaks are low except one at 29.53°. This peak occurs possibly due to doping of salts and MWCNTs filler in the PVA-PEG polymer blend. The occurrence of an intense peak in the 5 wt % sample is the result of aggregation of MWCNTs in this particular sample. From the available literature, it is confirmed that the addition of salt may bring some disorder in the polymeric chain structure and lead to a higher amorphous phase. However, the appearance of sharp peaks may be attributed to MWCNTs fillers in the polymer.[40−43]

3.2. FTIR Studies. The FTIR technique has been used to understand structural, microstructural and chemical structure variations in the intensity of the distinctive bands in the polymer composites.[44,45] The salt (NaNO$_3$) and polymer (PVA-PEG) interaction with filler MWCNTs has been investigated by using an FTIR spectrophotometer. The analysis of FTIR spectra of pure PVA, pure PEG, and blended PVA-PEG are discussed in the previous work of Sadiq et al.[51] The spectra and data of polymer blend PVA-PEG + NaNO$_3$ + x wt % of MWCNTs and attached functional groups are shown in Figure 3ii(a−d) and Table 1, respectively. In the FTIR spectra of the MWCNT-

Table 1. Band Assignments of FTIR Spectra for Polymer Blend (PVA-PEG)-NaNO$_3$ + x wt % of MWCNTs Containing Various Weight Percentages (x = 2.5, 5, 7. 5, and 10 wt %) Based Composite Electrolytes

x wt % of MWCNTs				
2.5 wt %	5 wt %	7.5 wt %	10 wt %	Band Assignments
838	832	843	841	CH$_2$ stretching
946	956	962	945	C−C stretching
1084	1087	1097	1092	−C−O stretching of PVA
1262	1250	1265	1245	C−H wagging/CH2 twisting
1356	1350	1311	1351	v1 (symmetric stretching mode/ CH$_2$ bending mode
1645	1645	1642	1637	C═C (st)
1728	1725	1728	1717	C−O stretching/vinyl ester of PVA
2920	2926	2946	2924	CH$_2$ asymmetric stretching/C−H stretching
3369	3378	3339	3381	O−H stretching

doped polymer blend the salt complex exhibits the peaks related to pure PVA, pure PEG, NaNO$_3$, and MWCNTs fillers and confirmed the formation of the composite.[46−49] The spectrum also confirmed the interaction between the polymer's functional group and the fillers. The IR absorbance peak at 3381 cm^{-1} corresponds to the respective bands of O−H stretching and N−H bonding. It is due to the stretching vibrations of the hydroxyl groups in PVA and the absorbed water molecules in PEG. This band represents intermolecular and intramolecular interactions involving PVA molecules and OH groups. There was a shift observed in the wavenumber of this band in MWCNTs samples which varies from 3369 to 3339 cm^{-1}.[50−53] The intermolecular and intramolecular interactions between OH groups in PVA and MWCNTs fillers are measured by the broadness of the OH band. There is also a similar fall in intensity for the weak and medium intensity bands at 843 and 841 cm^{-1}, respectively; this can be associated with CH$_2$ stretching. The C−O stretching and vinyl ester components of polyvinyl acetate (PVA) cause the band at 1717 cm^{-1} in the blend polymer, whereas the corresponding band in composite samples is found at a wavenumber in the range of 1725−1728 cm^{-1}. The band at 1642 cm^{-1} stands for the C═C stretching band. This band varies from 1637 to 1645 cm^{-1} in the case of CNT-doped PVA-PEG composites. The bands at 2946 and 2920 cm^{-1} correspond to CH$_2$ symmetric stretch and CH$_2$ asymmetric stretch, respectively. The absorbance mode of −C−O stretching of PVA peak at 1084 cm^{-1}. In the case of MWCNTs-doped composite films, the wavenumber changes from 1084 to 1092 cm^{-1} are due the complex formation between MWCNTs and the PVA-PEG polymer blend, which comes under the influence of intermolecular interactions within the polymer matrix.[54−60] The distinguishing feature in the polymer salt complex is that the

anion (NO_3^-) has IR modes at 1351 cm^{-1}. In view of the above results, we may conclude that MWCNT fillers interact with the PVA-PEG blend via a donor−acceptor pathway and enable the conduction process.

3.3. Raman Spectroscopy. Raman spectroscopy has been used to analyze carbon nanotube fillers and polymer blend composite electrolytes. The Raman spectra of a polymer blend composite augmented with carbon nanotube fillers revealed three distinct peaks as shown in Figure 3 iii (a−d). The first peak is a D band (1317 cm^{-1}) attributed to defects in MWCNT fillers and including sp^3-hybridized nanofillers. The second is an intensive G band (1592 cm^{-1}) attributed to tangential C−C bond stretching motion and shows the graphitic nature.[61] The final peak or 2D is a second order of the D band. It appears at 2656 cm^{-1} which is twice the frequency of the D band. We compared the intensities of the D and G bands to get the ID/IG ratio which is equal to 1.99 and reveals the defective nature. The stretching and deformation vibrations of CH_2 groups are linked to the bands at 2910 cm^{-1} in the PVA. Also, O−H group vibrations are responsible for the peak at 1086 cm^{-1}. In sp^2 carbon lattices, Raman spectroscopy can distinguish defects related to size, resulting in varied intensity ratios depending on the amount of disorder. However, the CH bond vibration peaks of 849 cm^{-1} may be contributed by C−C. The peak at 2606 cm^{-1} of PVA may arise due to the overlap of PEG on the PVA matrix.[62,63] The D-band peak is broadening due to the presence of sp^3 content and impurities in the polymer composite materials. Raman spectroscopy is an important tool to get the information about the disorder and defects in sp^2 carbon material. This information enables us to determine the intensity ratios depending on the amount of disorder. The calculated values of the intensity ratio, i.e., (ID/IG) bands, are presented in Table 2. ID/IG is used to detect the degree of defect.[64] In our

Table 2. Raman Spectra for Polymer Blend (PVA-PEG)-$NaNO_3$ + x wt % of MWCNTs Containing Various Weight Percentages (x = 2.5 wt %, 5 wt %, 7. 5 wt %, and 10 wt %) Based Composite Electrolytes

x wt % of CNTs	D-band (cm^{-1})	G-band (cm^{-1})	Intensity ratio, ID/IG
2.5	1317	1596	1.99
5	1320	1592	1.88
7.5	1328	1599	1.67
10	1313	1598	1.59

case, the intensity ratio decreases with the increase of CNT wt %. A decrease in ID/IG ratio indicates that defects in CNTs have decreased, and it represents the improvement in the graphitic nature.

3.4. Field Emission Scanning Electron Microscopy (FESEM). The FESEM was performed to obtain the surface morphology of the (PVA-PEG) + $NaNO_3$ with various weight percent of doped MWCNTs as shown in Figure 4i(a−d). The morphological structure of the dispersed types of composites shows the dispersion of MWCNTs in PVA-PEG blend matrix. The dispersion of CNTs is visible in the case of 2.5 wt % of filler, while in the case of 10 wt % filler we observe a rough surface in SEM image. This condition may arise due to higher concentration of filler and poor scanning by SEM. The morphology of polymer blend salt components is usually characterized by a semicrystalline pattern, and the presence of pores like texture structure confirm in the previous work of Sadiq et al.[51] At low concentrations (2.5 wt %) of the filler, the

microstructure is devoid of small pores that can modify the surface texture. The disappearance of pore and semicrystalline characteristics clearly shows the decrease in crystallinity of the sample.[65] At a higher concentration of 7.5 wt % of carbon nanotubes seems to be uniformly distributed in this polymer blend matrix. We can observe that the nanotubes are poorly dispersed in Figure 4i (b) because SEM cannot reveal the CNTs which are embedded inside the polymer matrix.[66] We know that CNTs have a covalent structure due to oxygen contained on the sidewall and PVA has a noncovalent structure. On this basis, we can say that PVA will contribute as the dispersant and matrix that formed the hydrogen bond with CNTs helps to yield a homogeneous distribution.[67−69] Figure 4i (d) shows the surface morphology of a 10 wt % polymer composite film which has a rough surface in comparison to other weight percentage samples of the composite films.

As a result, our MWCNTs-based BPCEs with a concentration of 10 wt % have stronger ionic conduction. Figure 4ii depicts the elemental distribution of MWCNTs in PBCEs. The polymer blend matrix is responsible for the presence of the carbon (C), oxygen (O), nitrogen (N), and sodium (Na) element. In general, the EDAX spectra Figure 4iii show the homogeneous distribution of MWCNTs in the PVA-PEG blend matrix. The atomic mass % for various elements are shown in Figure 4iv. Mapping of all existing elemental assignments of the polymer blend composite films for 10 wt % of MWCNTs contents is shown in Figure 4v. Consequently, it implies that MWCNTs fillers are homogeneously and evenly distributed and well diffused in the BPCE matrix and confirms the proper preparation of the solution by casting method.[70]

3.5. Thermal Properties. The DSC curves are used to study the thermal properties in polymeric materials such as glass transition, crystallization, melting, and decomposition processes which occur as the temperature of the sample rises according to a predetermined process. In the case of the PVA-PEG blend film, the melting peak located toward a lower temperature region which confirms a drop in average crystallite size and a lower degree of crystallinity.[71] Figure 5i(a−d) depicts the DSC curves of PVA-PEG + $NaNO_3$ + x wt % MWCNTs-based composite films (x = 2.5, 5,7.5, and 10 wt %). For all prepared polymer blend composite electrolytes, an endothermic peak (T_{m1}) has developed within a temperature range of 58−61 °C. Because PEG crystallizes around this temperature this peak can be attributed to melting of the PEG-rich phase.[72] The glass transition temperature is a critical characteristic for understanding polymer mix miscibility. The value of T_g for the blend system is determined by the structure and cooperative mobility of polymer chain segments., while for partially blended systems the value of T_g is taken from the individual polymer. Figure 5I shows the melting endotherm (T_{m2}) for all composite films prepared in the range of 187−195 °C and the decomposition endotherm (T_D) which is detected at 293 °C for composite films of 2.5 wt % which is comparatively larger than other fillers of different ratio. On addition of MWCNTs into the polymer matrix, the T_D values decrease which confirm, the intermolecular interaction between the polymer and fillers.[73,74] The TGA curves for blend polymers based pn PVA-PEG + $NaNO_3$ + x wt % of MWCNTs-based composite electrolytes (x = 2.5, 5, 7.5, and 10 wt %) are shown in Figure 5ii(a−d). The TGA curve demonstrates an initial weight loss in the 40−200 °C range. Another weight loss is observed in the 210−400 °C range. For pure PVA the thermal stability is shown to be around 320 °C, pure PEG shows thermal stability around 400 °C, and PVA-PEG
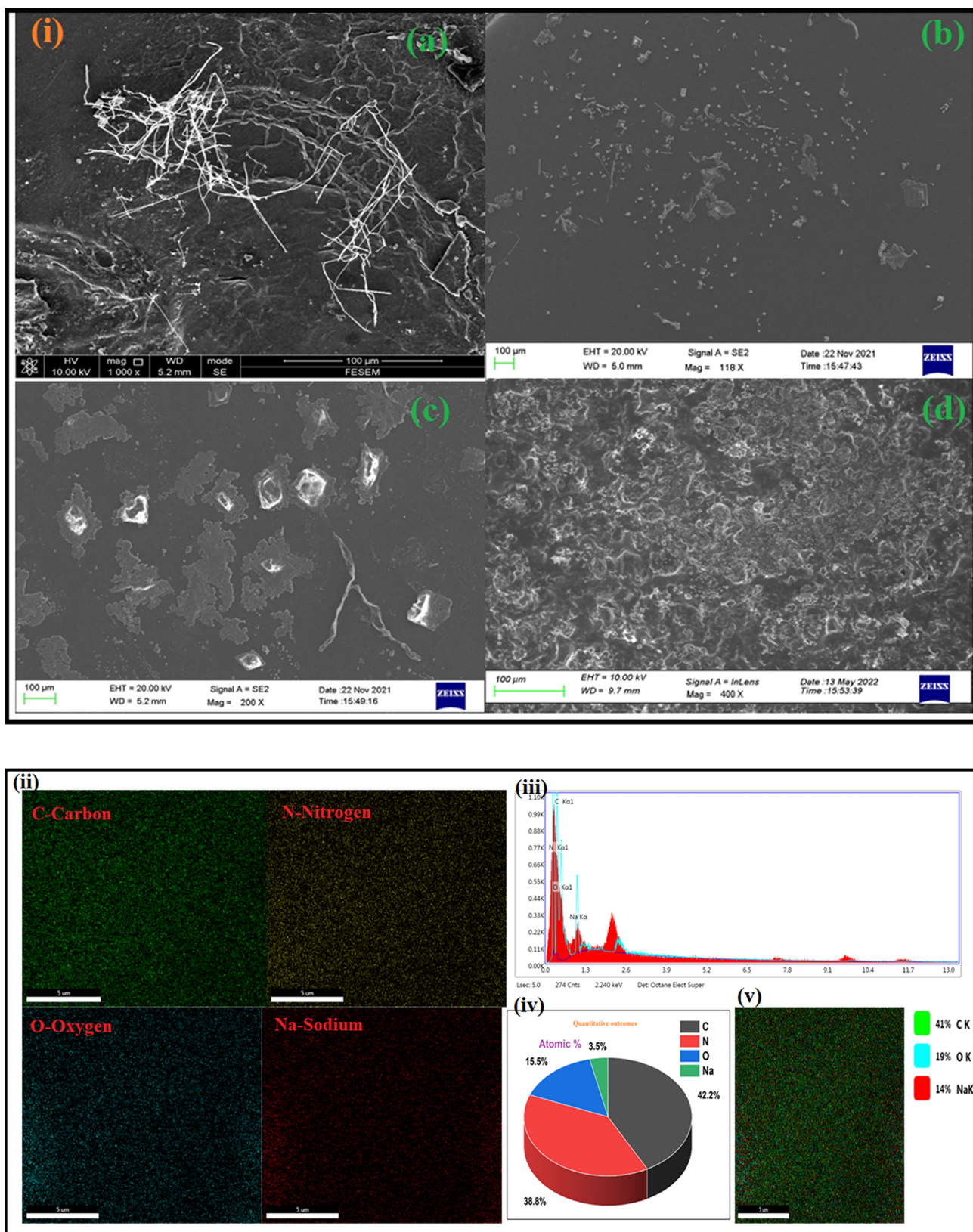
Figure 4. (i) FE-SEM images for various contents: (a) 2.5 wt %, (b) 5 wt %, (c) 7.5 wt %, and (d) 10 wt % of MWCNTs fillers. (ii) Mapping elements for various contents: 10 wt % of MWCNTs containing oxygen (O), nitrogen (N), carbon (C), and sodium (Na). (iii) EDAX analysis, (iv) atomic mass % for various elements, and (v) mapping of all existences by elemental assignment for 10 wt % of MWCNTs fillers.

blend polymer shows thermal stability 310 °C as reported in Sadiq et al.[51] The influence of filler on the polymer blend-salt matrix decreases the thermal stability, which is due to the leading

to polymeric backbone because of the disorder the bonding and thermal resistance of the polymers reported in Hirankumar et al.[75] The thermal stability of the polymer blend composite
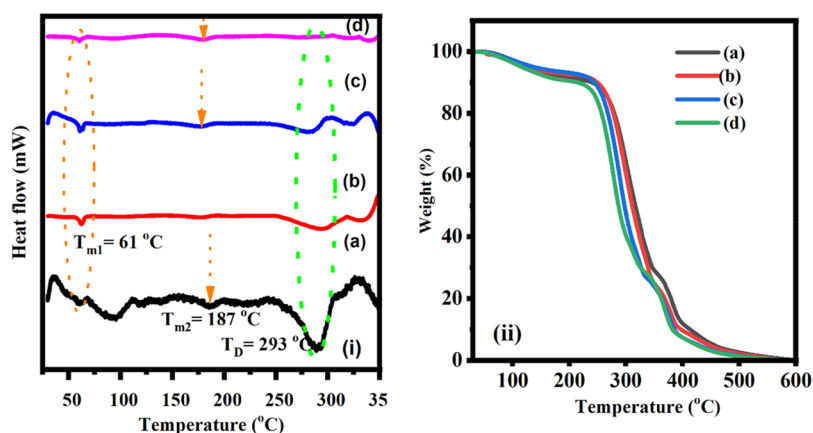
Figure 5. (i) DSC curves for various contents: (a) 2.5 wt %, (b) 5 wt %, (c) 7.5 wt %, and (d) 10 wt % of MWCNTs fillers. (ii) TGA curves for various contents: (a) 2.5 wt %, (b) 5 wt %, (c) 7.5 wt %, and (d) 10 wt % of MWCNTs fillers.
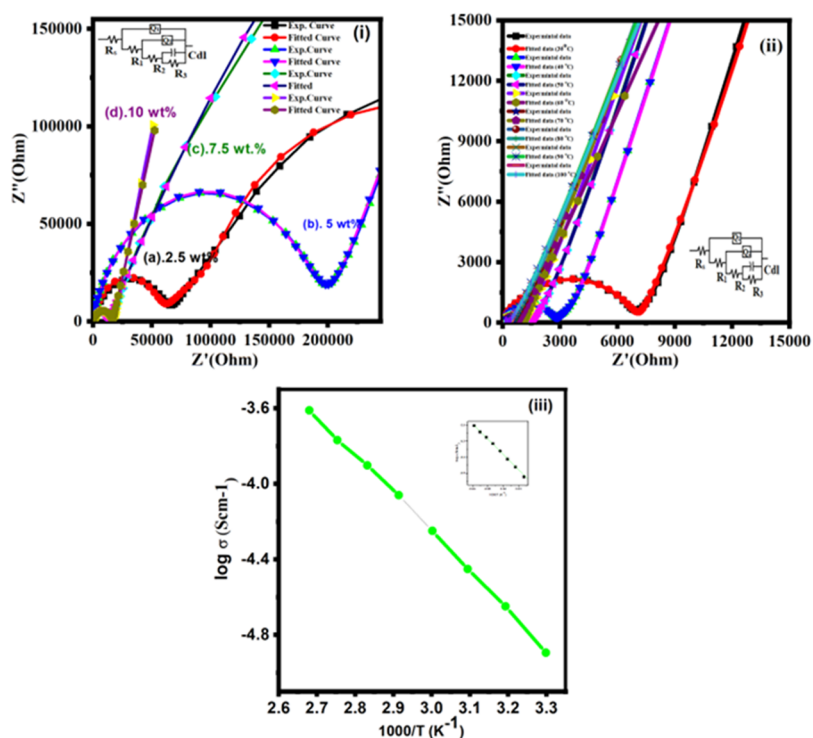
Figure 6. (i) Nyquist spectra for various contents: (a) 2.5 wt %, (b) 5 wt %, (c) 7.5 wt %, and (d) 10 wt % at 20 °C. (ii) Nyquist spectra for 10 wt % of MWCNTs at various temperatures. (iii) Arrhenius plot of highest conducting sample for 10 wt % of MWCNTs at various temperatures (30−100 °C).

electrolytes raises up to above 230 °C for the 7.5 wt % MWCNTs fillers. Consequently, standard polymer electrolyte is thermally more stable as compared with liquid electrolyte and favored when used in portable all solid-state electrochemical energy storage devices.[76,77] Therefore, the thermal stability of our prepared electrolytes is better for practical applications.

3.6. AC Impedance Spectroscopy. The AC-impedance spectra of polymer blend composites based on carbon nanotube are shown in Figure 6i. Nyquist plots contain the general characteristics at a high-frequency semiarc region followed by low-frequency spikes. The semiarc corresponds to the bulk characteristics of the system, and the low frequency peak corresponds to the charge build up at the electrode−electrolyte interface.[78−88] The obtained experimental data of impedance plots were fitted with an equivalent circuit model using Zsimp Win software. The experimental data perfectly fit with the theoretical model. The Chi-squared (χ^2, i.e., the sum of the squares of the differences between experimental data and theoretical data point) and relative errors were chosen as criteria for a satisfactory fit in the estimated parameters. The value of χ^2 was taken in between the range of 10^{-3} and 10^{-4}. The $R_s(Q_1(R_1(Q_2(R_2(CR_3)))))$ circuit model is used and shown in Figure 6,i,ii. The capacitance of the interfacial double layer (Cdl) is parallel to R_3. Electrolytic resistors (R_s) are connected in parallel with R_1, R_2, R_3, Q_1, and Q_2 of the constant phase element (CPE) and η is a fitting parameter dimensionless and its value is in the range of 0−1 to form the various circuit characteristics.[80,81] The electrical equivalent circuit parameters are shown in Table 3. Generally, PVA-PEG polymer blend is of insulating nature, and its electrical conductivity is 10^{-9} S/cm.[82] The Nyquist plots (Z'' vs Z') in the frequency range (10^{-1}−10^7) were examined at different temperatures (i.e., 20 and 100 °C). The conductivity of

Table 3. Impedance Spectra for Polymer Blend (PVA-PEG)-NaNO$_3$ + x wt % of MWCNTs Fillers Containing Various Weight Percentages (x = 2.5, 5, 7. 5, and 10 wt %) Based Composite Electrolytes for Different Parameter Values Extracted from the ZSimpWin Program to Fit the Equivalent Circuit Model of R$_s$(Q$_1$(R$_1$(Q$_2$(R$_2$(CR$_3$))))) at (a) 2.5 wt %, (b) 5 wt %, (c) 7.5 wt %, and (d) 10 wt %) of MWCNTs Filler Based Composite Electrolytes

Circuit component	x wt % of MWCNTs				
R$_s$(Q$_1$(R$_1$(Q$_2$(R$_2$(CR$_3$)))))	2.5 wt % (20 °C)	5 wt % (20 °C)	7.5 wt % (20 °C)	10 wt % (20 °C)	10 wt % (100 °C)
R_s/Ω	3.252×10^{-6}	13.58	1.032×10^{-7}	19.87	58.05
$Q_1/Y_o(\mu S \times s^{-n})$	3.546×10^{-10}	1.117×10^{-11}	4.065×10^{-10}	5.527×10^{-9}	6.766×10^{-9}
η	0.825	0.99	0.8348	0.7252	0.7802
R_1/Ω	5.821×10^4	2.545×10^4	1.33×10^4	1.687E4	274.7
$Q_2/Y_o(\mu S \times s^{-n})$	9.174×10^{-7}	1.706×10^{-9}	1.884×10^{-6}	2.873×10^{-6}	7.239×10^{-5}
η	0.504	0.656	0.634	0.7777	0.5427
R_2/Ω	1.305×10^5	1.728×10^5	1.643×10^6	3.736E11	743.6
Cdl/F	1.085×10^{-7}	1.317×10^{-6}	1.369×10^{-7}	9.745×10^9	2.192×10^{-8}
R_3/Ω	3.501×10^5	7.964×10^5	8.339×10^9	1.197×10^6	0.4787
χ^2	8.915×10^{-3}	8.321×10^{-3}	8.860×10^{-3}	3.059×10^{-7}	4.664×10^{-4}
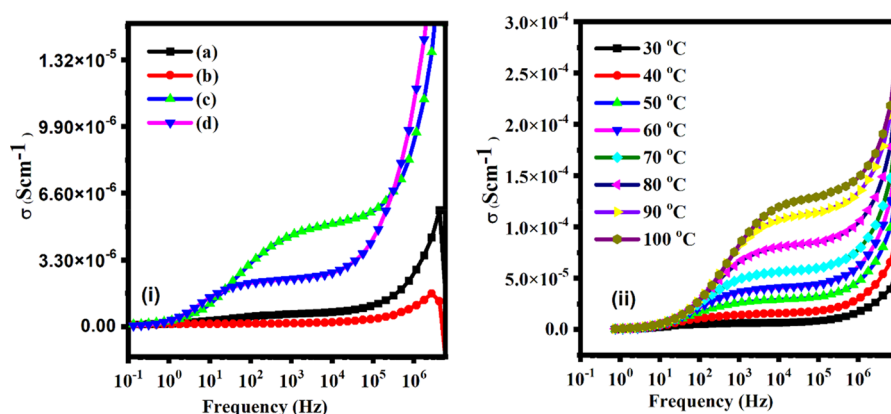
Figure 7. (i) AC conductivity spectra against frequency (Hz) for various contents: (a) 2.5 wt %, (b) 5 wt %, (c) 7.5 wt %, and (d) 10 wt % of MWCNTs fillers at 20 °C. (ii) A.C. conductivity spectra with frequency (Hz) for 10 wt % of MWCNTs at various temperatures.

the prepared polymer blend composite electrolyte is calculated using the following formula.

$$\sigma = \frac{P}{R_b \times s} \qquad (1)$$

Here, P is the thickness of PBCEs, S is the surface area of PBCEs, and R$_b$ is the bulk resistance.[83] R$_b$ (bulk resistance) value is determined on the x-axis of the Nyquist plots, and the obtained conductivity result is summarized in below Table 5. The 10 wt % of MWCNTs concentration increases the conductivity of the composite to 4.32×10^{-6} S/cm at 20 °C. Figure 6(ii) depicts the relationship between ionic conductivity and various temperatures. The highest electrical conductivity (2.253×10^{-4} S cm^{-1}) has been achieved at 100 °C.

The temperature versus log σ plot follows the behavior of the Arrhenius equation,

$$\sigma = A \exp\left(-\frac{E_a}{kT}\right) \qquad (2)$$

Here, A is the pre-exponential factor, E_a is the activation energy, k is the Boltzmann constant (1.38×10^{-23} J/K), and T is the temperature in Kelvin. The plot log σ and $1000/T$ reveals the linear relationship between them as shown in Figure 6iii. From the linear fitting methods, we obtain the activation energy (E_a) values of 0.41 eV, respectively. The activation energy is the sum of the generation and migration energies of mobile charge carriers.[84,85] In general, a polymer electrolyte with a low

activation energy will have a high ionic conductivity which is desirable for practical applications.

3.7. Dielectric Investigations. *3.7.1. AC impedance spectra.* The AC-conductivity of PVA-PEG + NaNO$_3$ + x wt % of MWCNTs (x = 2.5, 5, 7.5, and 10 wt %) samples is plotted against frequency at 20 °C (Figure 7i) and at different temperatures in the range of 30−100 °C (Figure 7ii). The AC conductivity was calculated from dielectric data using the formula

$$\sigma_{ac} = \omega \varepsilon_0 \varepsilon_r \tan \delta \qquad (3)$$

where tan δ is the loss tangent and the AC impedance measures the σ_{ac}. Figure 7i,ii shows three regions. At low frequency there is increase in conductivity with an increase of frequency followed by a frequency-independent region, and the DC conductivity is extracted from it. At high frequency the continuous increase in frequency corresponds to the dispersion region.[86] It may be noted that ionic conductivity increases with temperature and suggests the thermal activation of charge carriers. An increase of temperature enhances the segmental motion of polymer chain and, hence, faster ion transport.[87] The direct relationship between temperature and ionic conductivity is simply explained in terms of hopping mechanisms between coordination sites and movement of the polymer−salt−filler matrix component. As a result of the internal polymer chain, it rises rapidly with the temperature enhancement and promotes ionic mobility between
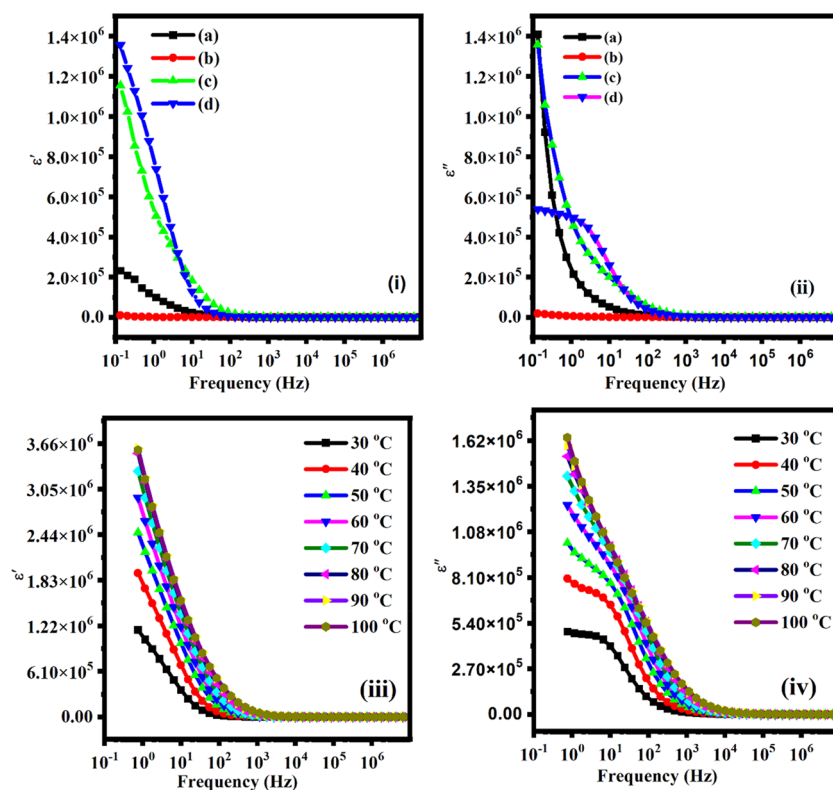
Figure 8. (i) Dielectric constant (ε') and (iii) dielectric loss (ε'') against frequency for various contents: (a) 2.5 wt %, (b) 5 wt %, (c) 7.5 wt %, and (d) 10 wt % of MWCNTs fillers at 20 °C. (ii) Dielectric constant (ε') and (iv) dielectric loss (ε'') with frequency for 10 wt % of MWCNTs fillers at various temperatures.

and within the matrix which improves the ionic conductivity of the polymer blend composite electrolyte.[88,89]

3.7.2. Dielectric Constant and Dielectric Loss. The complex dielectric properties such dielectric constant (ε') and the dielectric loss (ε'') of the polymer blend composite electrolytes are studied by the impedance spectroscopy. The mathematical expression the real part and imaginary part of complex permittivity can be expressed as

$$\begin{cases} \varepsilon^* = \varepsilon' - i\varepsilon'' \\ \varepsilon' = \dfrac{-Z''}{\omega C_o(Z'^2 + Z''^2)} \\ \varepsilon'' = \dfrac{Z'}{\omega C_o(Z'^2 + Z''^2)} \end{cases} \tag{4}$$

where Z' and Z'' are the real and imaginary parts of the impedance. C_o is the capacitance, and ω is the angular frequency.[90] Figure 8i,iii depicts the frequency dependence of real and imaginary part of the dielectric constant and dielectric loss behavior at 20 °C temperature and similar in Figure 8ii,iv show the frequency dependence of real and imaginary part of the dielectric constant and dielectric loss behavior at various temperature.

As per the spectra of the dielectric constant (ε') and dielectric loss (ε'') it is clearly seen that their values reduced with respect to the frequency it may be due to the reduction in the space charge by the orientation of the dipole in the direction of the applied electric field. At high frequency the dielectric constant (ε') and dielectric loss (ε'') become minimal due to the lack of charge accumulation at the electrolyte–electrode interface.[87,88] We observed the high dielectric constant (ε') value at low

frequencies that may be due to the electrode polarization effect where the dipoles are oriented in the direction of the applied electric field. Figure 8iii,iv shows the temperature-dependent dielectric constant and dielectric loss as the frequency for the sample (10 wt %) at various temperatures. In the low frequency region, on increasing the temperature the dielectric constant and loss both are increased it may be due to the induction of space charge by the thermal activation phenomena and formation of dipoles which induced the polarization effect at the electrode–electrolyte interface.[89,90] At high frequency the dielectric constant and loss reduced drastically because high field aligned the dipoles and reduced the space charge effect by the fast movement of ions through the electrolyte–electrode interface.[91−96] When the temperature rises, the ion-pair dissociation process increases as well as the free carrier density at the interface increases. We know that the conductivity is highly influenced by temperature; hence, dielectric loss increases as the temperature increases. This thermal activation of charge carriers results in enhance polarization and, hence, dielectric constant (ε'). Therefore, an increase in dielectric loss (ε'') leads to hopping of charge carriers in the polymer electrolytes.

3.7.3. Electric Module. The electric module behavior has been studied by using the formula

$$\begin{cases} M^* = M' + iM'' \\ M'' = \dfrac{\varepsilon'}{(\varepsilon')^2 + (\varepsilon'')^2} = \omega C_o Z'' \\ M'' = \dfrac{\varepsilon''}{(\varepsilon')^2 + (\varepsilon'')^2} = \omega C_o Z' \end{cases} \tag{5}$$
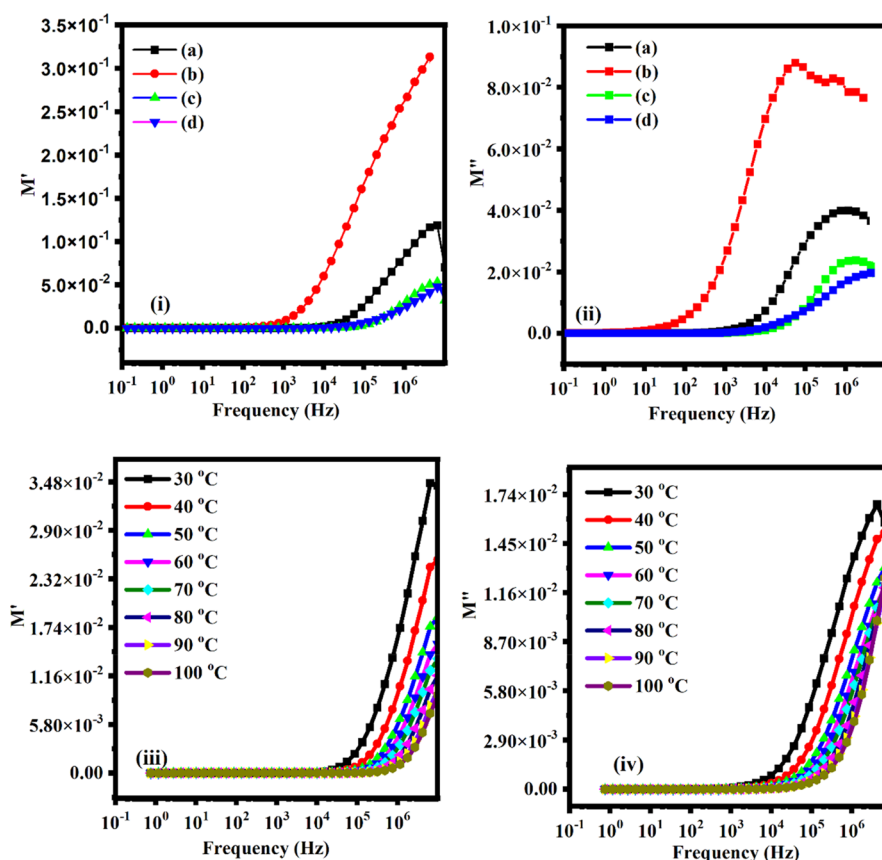
Figure 9. (i) Real part (M′) and (ii) Imaginary part (M′′) of electric modulus against frequency (Hz) for various contents: (a) 2.5 wt %, (b) 5 wt %, (c) 7.5 wt %, and (d) 10 wt % of MWCNTs fillers at 20 °C. (iii) Real part (M′) and (iv) imaginary part (M′′) of electric modulus with frequency (Hz) for 10 wt % of MWCNTs fillers at various temperatures.
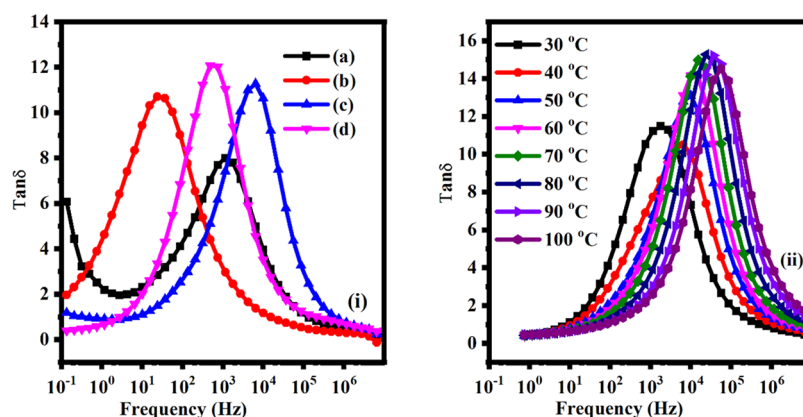
Figure 10. (i) tan δ against frequency for various contents: (a) 2.5 wt %, (b) 5 wt %, (c) 7.5 wt %, and (d) 10 wt % of MWCNT fillers at 20 °C. (ii) tan δ with frequency for 10 wt % of MWCNTs fillers at various temperatures.

where $M′$ and $M′′$ are the real and imaginary parts of electric modulus, ω is the angular frequency, C_o is the capacitance of the dielectric material and $Z′$ and $Z′′$ are the real and imaginary parts of the impedance.[97] Since both the value $M′$ (see Figure 9i) and $M′′$ (see inset of Figure 9ii) are very close to zero at the lower frequency side which shows the migration of ions in polymer/polymer-blend and $M′$ (i.e., $= \omega C_o Z′′$) and $M′′$ (i.e., $= \omega C_o Z \omega C_o Z′$), both shifts toward higher frequency side with increasing temperature (i.e., the motion of ions became faster and hence charge carriers are thermally activated) and MWCNTs fillers, although, the values of $M′$ and $M′′$ both are very close to zero at lower frequency and increase at higher

frequency. The occurrence of peaks occurs in the modulus formalism (at higher frequencies for all polymer-blend systems) and temperatures because of the localized motion of ions as shown in Figure 9iii,iv. At lower frequency region the values of $M′$ and $M′′$ specify the negligible electrode polarization.[98,99] In addition, the appearance of a long tail at the lower frequency side shows that the electrodes might be associated with large capacitance. The smaller value of $M′$ (at lower frequency side) confirms that no any involvement of electrode polarization (followed by continuous dispersion on increasing frequency due to conductivity relaxation phenomenon). This is because of the lack of restoring force governing the mobility of charge carriers

Table 4. Values of Relaxation Time for Polymer Blend (PVA-PEG)-NaNO$_3$ + x wt % of MWCNTs Containing Various Weight Percentages (x = 2.5, 5, 7. 5, and 10 wt %) Based Composite Electrolytes at 20 °C and Highest Conducting Sample x = 10 wt % of MWCNTs Fillers at Various Temperatures

Sample concentration x wt % of MWCNTs (20 °C)	Angular frequency (ω_{max})	Relaxation time (τ, s)	Highest conducting (10 wt %) sample		
			Temp (°C)	Angular frequency (ω_{max})	Relaxation time (τ, s)
2.5 wt %	1303.01	7.67×10^{-4}	30	1904.30	5.25×10^{-4}
			40	6709.30	1.49×10^{-4}
5 wt %	33.37	2.99×10^{-2}	50	10513.31	9.51×10^{-5}
			60	13512.83	7.40×10^{-5}
7.5 wt %	6448.61	1.55×10^{-4}	70	15974.11	6.26×10^{-5}
			80	24702.45	4.04×10^{-5}
10 wt %	664.41	1.50×10^{-3}	90	40808.40	2.45×10^{-5}
			100	62279.21	6.60×10^{-5}
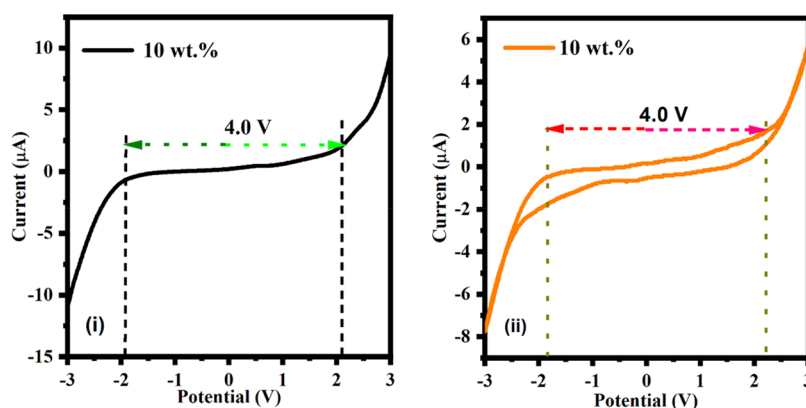
Figure 11. (i) Linear voltammetry curve of polymer blend composite electrolytes at 10 wt % of MWCNT fillers. (ii) Cyclic voltammetry curve of polymer blend composite electrolytes at 10 wt % of MWCNTs fillers.

under the influence of steady electric field.[100] From the above observations, we can say that the addition of MWCNTs in polymer/polymer-blend system increases the amorphous phase in the polymer matrix. This relaxation process existed in higher frequency region may be due to increased flexibility of host matrix.

3.7.4. Tangent Delta. The dielectric behavior of the polymer blend composite electrolytes plotted against frequency is shown in Figure 10i,ii. The mathematical expression for tan (δ) is given by eq 6.

$$\begin{cases} \varepsilon'' = \varepsilon' \tan \delta \\ \tan \delta = \dfrac{\varepsilon''}{\varepsilon'} \end{cases} \tag{6}$$

From Figure 10i, it can be found that the shift in relaxation peaks toward higher frequency with an increase in the MWCNTs concentrations into PBCEs films.[101−104] Although Figure 10ii shows temperature-dependent tan δ against a frequency (Hz) plot for the sample containing 10 wt % of MWCNTs which exhibits a frequency shift with temperature (from 30 to 100 °C) the relaxation peaks shift toward higher frequency regions. This shift in relaxation frequency may due to increased segmental motion of the polymeric chains. Therefore, it favors the conduction of ion inside the matrix of polymer, i.e., thermally activated behavior of dielectric polarization. Also, the tangent delta is powerfully impacted by the ions because of the existence orientation of dipole into the polymeric matrix and hence to the ionic conductivity (which can also be seen in the relaxation time). Furthermore, the maximum value of tangent

delta against frequency can be determined by using the relation $\omega\tau = 1$ where ω and τ, respectively, are the angular frequency and relaxation time.[105−107] The relaxation time ($\tau = 1/(2\pi f max)$ has also been calculated as presented in Table 4 and obtained as a minimum relaxation time for PBCEs films having 10 wt % MWCNTs content and a maximum for the sample containing 10 wt % MWCNTs. The decrease in the dielectric loss tangent relaxation process and a reduction in relaxation time signify less hindrance in the segmental dynamics of polymeric chains (i.e., conductivity relaxation).[108−110] This finding is most favorable to the result of dielectric permittivity as already discussed.

3.8. Electrochemical Performance. The electrochemical stability of polymer blend composite electrolytes was performed by the linear sweep voltammetry (LSV) technique. The highest conducting sample (i.e., 10 wt %) composite electrolytes operating within the potential range (−3 to +3) V under a scan rate of 10 mV/s are presented in Figure 11i. The maximum operating potential range of the electrolyte, i.e., the decomposition potential, is 4.0 V of the PBCEs at 30 °C. It has been observed that the current remained constant initially and then rapidly increased. This phenomenon occurs due to the electrolyte breakdown at the inert electrode contact.[111,112]

The highest conducting sample of blend polymer composite film is 10 wt % and was scanned at a rate of 10 mV/s at 30 °C within the potential range of −3 to +3 V. The cyclic voltammetry (CV) plot is shown in Figure 11ii. The absence of cathodic and anodic peaks can be seen in voltammograms throughout the cycles.[113,114] Furthermore, after one cycle, the polymer electrolyte's stability remains the same and its stability window is up to 4.0 V which establishes it as a promising candidate to use
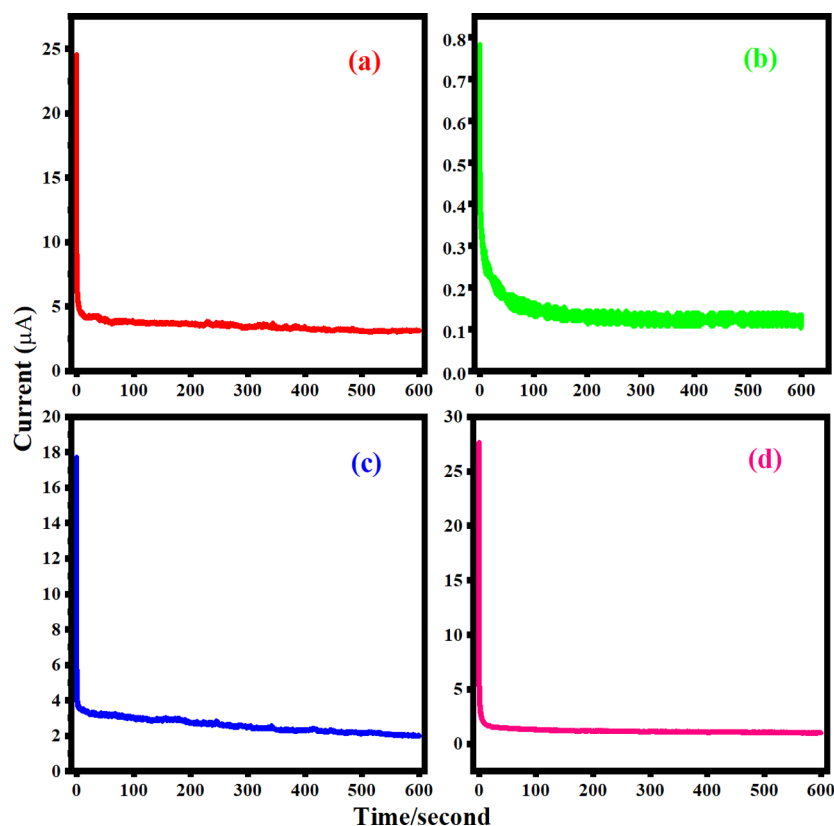
Figure 12. Constant current vs time (s) for various contents: (a) 2.5 wt %, (b) 5 wt %, (c) 7.5 wt %, and (d) 10 wt % of MWCNTs fillers at room temperature.

Table 5. Electrical Conductivity and Transference Number Measurement for Polymer Blend (PVA-PEG)-NaNO$_3$ + x wt % MWCNTs Containing Various Weight Percentages (x = 2.5, 5, 7. 5, and 10 wt %) Based Composite Electrolytes

		Transport no.		Conductivity (S cm^{-1})	
x wt % of MWCNTs	Electrical conductivity (S cm^{-1}) 20 °C	t_{ion}	t_{ele}	σ_{ionic}(S cm^{-1})	$\sigma_{electronic}$(S cm^{-1})
2.5 wt %	4.989×10^{-7}	0.868	0.132	4.33×10^{-7}	6.65×10^{-8}
5 wt %	1.02×10^{-7}	0.845	0.156	8.86×10^{-8}	1.59×10^{-8}
7.5 wt %	3.59×10^{-6}	0.879	0.112	3.15×10^{-6}	4.02×10^{-7}
10 wt %	4.32×10^{-6}	0.968	0.035	4.21×10^{-6}	1.51×10^{-7}

in the electrochemical devices, electrochemical double layer capacitors, and sodium ion battery applications.

3.9. Chronoamperometry (CA) Studies. The DC polarization technique was used to quantify the transference number of ions (t_{ion}) and electrons (t_{ele}) at a potential of 2 V for 600 s. Figure 12 depicts the results of the measurements. As the mobile ions at the electrode/electrolyte contact are polarized, the peak current diminishes instantly. The current usually approaches zero for pure ionic conductors or reaches a constant residual value for mixed ionic and electronic conductors. The initial current (I_i) is caused either by ions or by a combination of ionic and electronic conduction, whereas the constant residual current is caused solely by electron conduction. The polarization current vs time data was used to calculate the transference numbers for ions (t_{ion}) and electrons (t_{ele}) of PBCEs films which can be calculated by using the equation as

$$\begin{cases} t_{ion} = \left(\dfrac{I_i - I_f}{I_i} \right) \\ t_{elec} = \left(\dfrac{I_f}{I_i} \right) \end{cases} \tag{7}$$

where I_i(solely due to ions) and I_f (due to electrons/ions) denote the starting and ending currents, respectively, at times t_i and time t_f. The contribution of ionic and electronic conductivity is calculated by the expression given in eq 8.

$$i_t = i_{ion} + i_{ele} \tag{8}$$

The contribution of ionic conductivity and electronic conductivity in the PBCEs films was also estimated by using the following relationship.[115,116]

$$\begin{cases} \sigma_{ionic} = \sigma_{electrical} \times t_{ion} \\ \sigma_{electronic} = \sigma_{electrical} \times t_{electronic} \end{cases} \tag{9}$$

The maximum transference number of ion (t_{ion}) was 0.968 for 10 wt %, and the transference number of electronic t_{elec} is 0.035

for the 10 wt % sample. The estimated values of transference number and their corresponding electrical conductivity are given in Table 5. Table 5 shows that the ionic transference number is nearly ~1 and does not change significantly with salinity. Above that, the increased mobility of electron may be because there is no possibility of formation of ion clusters. Therefore, the mechanism of charge transport into the prepared PBCEs electrolyte films is predominantly due to ions.

4. CONCLUSION

Using the solution standard casting technique, we prepared polymer blend composite electrolytes based on (PVA-PEG) + $NaNO_3$ + x wt% of MWCNTs (where x = 2.5, 5, 7.5, and 10 wt % of MWCNTs fillers). X-ray diffraction spectra and FESEM confirm the formation of polymer composites. FTIR and Raman spectroscopy confirmed the presence of structural-phase formations and the interactions between polymers, salt, MWCNTs, and ions. Surface morphology of the prepared polymer blend composite electrolytes was analyzed by using FESEM. The thermal properties of the PBCE films were effectively determined by DSC. The ionic conductivity was obtained in the case of 10 wt % of MWCNTs filler which is equal to 4.32×10^{-6} S cm^{-1} at 20 °C. At higher temperature, the enhancement in ionic conductivity has been observed. The obtained value is 2.253×10^{-4} S/cm at 100 °C. AC conductivity, dielectric properties, and tan δ values were effectively obtained through an impedance spectroscopy. The dielectric constant, dielectric loss, and loss tangent values were found to rise due to its dependence on temperature and frequency. In addition, the highest conductivity sample is checked with linear sweep voltammetry (LSV) and cyclic voltammetry (CV) approaches was used to calculate the potential window. The voltage stability is found to be 4.0 V at room temperature for 10 wt % of MWCNTs. The cyclic voltammetry (CV) technique has been used to identify and make sure that there is no single oxidation and reduction peak in the polymer blend composite electrolytes. These finding are important and suggest that the device is suited for EDLC supercapacitors, Na-battery, Li-battery, fuel cells, and other energy applications.

■ AUTHOR INFORMATION

Corresponding Author

Javid Ali − *Department of Physics, Jamia Millia Islamia (A Central University), New Delhi 110025, India;* ⊙ orcid.org/0000-0001-8042-8733; Email: javi_reslab@rediffmail.com

Authors

Mohd Sadiq − *Department of Physics, Jamia Millia Islamia (A Central University), New Delhi 110025, India; Department of Physics, A. R. S. D College, University of Delhi, New Delhi 110021, India*

M. Ajmal Khan − *Department of Physics, Jamia Millia Islamia (A Central University), New Delhi 110025, India*

Mohammad Moeen Hasan Raza − *Department of Physics, Jamia Millia Islamia (A Central University), New Delhi 110025, India;* ⊙ orcid.org/0000-0002-5898-7106

Shah Masheerul Aalam − *Department of Physics, Jamia Millia Islamia (A Central University), New Delhi 110025, India*

Mohammad Zulfequar − *Department of Physics, Jamia Millia Islamia (A Central University), New Delhi 110025, India*

Complete contact information is available at:
https://pubs.acs.org/10.1021/acsomega.2c04933

■ REFERENCES

(1) Ngai, K. S.; Ramesh, S.; Ramesh, K.; Juan, J. C. A review of polymer electrolytes: fundamental, approaches and applications. *Ionics.* **2016**, *22*, 1259−79.

(2) Wong, J. I.; Ramesh, S.; Jun, H. K.; Liew, C. W. Development of poly (vinyl alcohol) (PVA)-based sodium ion conductors for electric double-layer capacitors application. *Materials Science and Engineering: B* **2021**, *263*, 114804.

(3) Arya, A.; Sharma, A. L. A glimpse on all-solid-state Li-ion battery (ASSLIB) performance based on novel solid polymer electrolytes: a topical review. *J. Mater. Sci.* **2020**, *55*, 6242−304.

(4) Wu, N.; Chien, P. H.; Li, Y.; Dolocan, A.; Xu, H.; Xu, B.; Grundish, N. S.; Jin, H.; Hu, Y. Y.; Goodenough, J. B. Fast Li$^+$ conduction mechanism and interfacial chemistry of a NASICON/polymer composite electrolyte. *J. Am. Chem. Soc.* **2020**, *142*, 2497−505.

(5) Li, S.; Zhang, S. Q.; Shen, L.; Liu, Q.; Ma, J. B.; Lv, W.; He, Y. B.; Yang, Q. H. Progress and perspective of ceramic/polymer composite solid electrolytes for lithium batteries. *Advanced Science.* **2020**, *7*, 1903088.

(6) Zhang, Z.; Zhang, Q.; Ren, C.; Luo, F.; Ma, Q.; Hu, Y. S.; Zhou, Z.; Li, H.; Huang, X.; Chen, L. A ceramic/polymer composite solid electrolyte for sodium batteries. *Journal of Materials Chemistry A* **2016**, *4*, 15823−8.

(7) Arya, A.; Sharma, A. L. Polymer electrolytes for lithium-ion batteries: a critical study. *Ionics.* **2017**, *23*, 497−540.

(8) Qazi, R. A.; Ali Shah, L.; Ullah, R.; Khattak, R.; Sadiq, M.; Saleem Khan, M. Synthesis, characterization, and ammonia sensing performance of poly (3-hydroxybutyrate) grafted multiwall carbon nanotubes. *Polymer-Plastics Technology and Materials* **2022**, *61* (1), 93−106.

(9) Alipoori, S.; Mazinani, S.; Aboutalebi, S. H.; Sharif, F. Review of PVA-based gel polymer electrolytes in flexible solid-state supercapacitors: Opportunities and challenges. *journal of energy storage.* **2020**, *27*, 101072.

(10) Abdulwahid, R. T.; Aziz, S. B.; Kadir, M. F. Insights into ion transport in biodegradable solid polymer blend electrolyte based on FTIR analysis and circuit design. *J. Phys. Chem. Solids* **2022**, *167*, 110774.

(11) Asadpour, S.; Raeisi, A.; Kooravand, M.; Asfaram, A. A review on zinc oxide/poly (vinyl alcohol) nanocomposites: Synthesis, characterization and applications. *Journal of Cleaner Production.* **2022**, *362*, 132297.

(12) Reddy, P. L.; Deshmukh, K.; Chidambaram, K.; Ali, M. M.; Sadasivuni, K. K.; Kumar, Y. R.; Lakshmipathy, R.; Pasha, S. K. Dielectric properties of polyvinyl alcohol (PVA) nanocomposites filled with green synthesized zinc sulphide (ZnS) nanoparticles. *Journal of Materials Science: Materials in Electronics.* **2019**, *30*, 4676−87.

(13) Wang, Z.; Zhu, M.; Pei, Z.; Xue, Q.; Li, H.; Huang, Y.; Zhi, C. Polymers for supercapacitors: boosting the development of the flexible and wearable energy storage. *Materials Science and Engineering: R: Reports.* **2020**, *139*, 100520.

(14) Zhao, L.; Fu, J.; Du, Z.; Jia, X.; Qu, Y.; Yu, F.; Du, J.; Chen, Y. High-strength and flexible cellulose/PEG based gel polymer electrolyte with high performance for lithium ion batteries. *J. Membr. Sci.* **2020**, *593*, 117428.

(15) Bharati, D. C.; Kumar, H.; Saroj, A. L. Chitosan-PEG-NaI based bio-polymer electrolytes: structural, thermal and ion dynamics studies. *Materials Research Express.* **2019**, *6*, 125360.

(16) Mousa, E.; Hafez, Y.; Nasr, G. M. Optical Study on PVA/PEG Blend Doped with Nano-Silica. *J. Electron. Mater.* **2021**, *50*, 2594−604.

(17) El Nemr, A.; Serag, E.; El-Maghraby, A.; Fathy, S. A.; Abdel Hamid, F. F. Manufacturing of pH sensitive PVA/PVP/MWCNT and PVA/PEG/MWCNT nanocomposites: an approach for significant drug release. *Journal of Macromolecular Science, Part A* **2019**, *56*, 781−93.

(18) Du, J.; Bai, J.; Cheng, H. The present status and key problems of carbon nanotube based polymer composites. *Express Polymer Letters.* **2007**, *1*, 253−73.

(19) Tarfaoui, M.; Lafdi, K.; El Moumen, A. Mechanical properties of carbon nanotubes based polymer composites. *Composites Part B: Engineering.* **2016**, *103*, 113−21.

(20) Yang, Z.; Xu, D.; Liu, J.; Liu, J.; Li, L.; Zhang, L.; Lv, J. Fabrication and characterization of poly (vinyl alcohol)/carbon nanotube melt-spinning composites fiber. *Progress in Natural Science: Materials International.* **2015**, *25*, 437−44.

(21) Hasan, M.; Das, S. K.; Islam, J. M.; Gafur, M. A.; Hoque, E.; Khan, M. A. Thermal properties of carbon nanotube (CNT) reinforced polyvinyl alcohol (PVA) composites. *International Letters of Chemistry, Physics and Astronomy* **2013**, *12*.

(22) Yee, M. J.; Mubarak, N. M.; Khalid, M.; Abdullah, E. C.; Jagadish, P. Synthesis of polyvinyl alcohol (PVA) infiltrated MWCNTs buckypaper for strain sensing application. *Scientific reports.* **2018**, *8*, 1−6.

(23) Molnár, K.; Košťáková, E.; Mészáros, L. Electrospinning of PVA/carbon nanotube composite nanofibers: the effect of processing parameters. *In Materials Science Forum* **2008**, *589*, 221−226.

(24) Mallakpour, S.; Ezhieh, A. N. Preparation and characterization of chitosan-poly (vinyl alcohol) nanocomposite films embedded with functionalized multi-walled carbon nanotube. *Carbohydrate polymers.* **2017**, *166*, 377−86.

(25) Mombini, S.; Mohammadnejad, J.; Bakhshandeh, B.; Narmani, A.; Nourmohammadi, J.; Vahdat, S.; Zirak, S. Chitosan-PVA-CNT nanofibers as electrically conductive scaffolds for cardiovascular tissue engineering. *International journal of biological macromolecules.* **2019**, *140*, 278−87.

(26) Portillo-Rodríguez, B.; Sanchez-Vasquez, J. D.; Reyes-Reyes, M.; Lopez-Sandoval, R. The effect of the PVA hydrolysis degree on the electrical properties of organic resistive memories based on PVA+ CNT composites. *Diamond Relat. Mater.* **2022**, *121*, 108720.

(27) Xue, P.; Park, K. H.; Tao, X. M.; Chen, W.; Cheng, X. Y. Electrically conductive yarns based on PVA/carbon nanotubes. *Composite Structures.* **2007**, *78*, 271−7.

(28) Zhang, L.; Xu, W.; Luo, X. G.; Wang, J. N. High performance carbon nanotube based composite film from layer-by-layer deposition. *Carbon.* **2015**, *90*, 215−21.

(29) Zhou, Q.; Chen, T.; Cao, S.; Xia, X.; Bi, Y.; Xiao, X. A novel flexible piezoresistive pressure sensor based on PVDF/PVA-CNTs electrospun composite film. *Appl. Phys. A: Mater. Sci. Process.* **2021**, *127*, 1−0.

(30) Cadek, M.; Coleman, J. N.; Barron, V.; Hedicke, K.; Blau, W. J. Morphological and mechanical properties of carbon-nanotube-reinforced semicrystalline and amorphous polymer composites. *Applied physics letters.* **2002**, *81*, 5123−5.

(31) Pour, G. B.; Aval, L. F.; Mirzaee, M. CNTs Supercapacitor Based on the PVDF/PVA Gel Electrolytes. *Recent Patents on Nanotechnology.* **2020**, *14*, 163−70.

(32) Tsai, Y. C.; Huang, J. D.; Chiu, C. C. Amperometric ethanol biosensor based on poly (vinyl alcohol)-multiwalled carbon nanotube-alcohol dehydrogenase biocomposite. *Biosensors and Bioelectronics.* **2007**, *22*, 3051−6.

(33) Nath, B. C.; Gogoi, B.; Boruah, M.; Khannam, M.; Ahmed, G. A.; Dolui, S. K. High performance polyvinyl alcohol/multi walled carbon nanotube/polyaniline hydrogel (PVA/MWCNT/PAni) based dye sensitized solar cells. *Electrochim. Acta* **2014**, *146*, 106−11.

(34) Jhang, J. C.; Lin, J. H.; Lou, C. W.; Chen, Y. S. Biodegradable and conductive PVA/CNT nanofibrous membranes used in nerve conduit applications. *Journal of Industrial Textiles* **2021**, 152808378211032086.

(35) Agrawal, S. L.; Rai, N.; Natarajan, T. S.; Chand, N. Electrical characterization of PVA-based nanocomposite electrolyte nanofibre mats doped with a multiwalled carbon nanotube. *Ionics.* **2013**, *19*, 145−54.

(36) Pritam; Arya, A.; Sharma, A. L. Selection of best composition of Na+ ion conducting PEO-PEI blend solid polymer electrolyte based on structural, electrical, and dielectric spectroscopic analysis. *Ionics.* **2020**, *26*, 745−66.

(37) Li, W.; Xu, F.; Sun, L.; Liu, W.; Qiu, Y. A novel flexible humidity switch material based on multi-walled carbon nanotube/polyvinyl alcohol composite yarn. *Sensors and Actuators B: Chemical.* **2016**, *230*, 528−35.

(38) Malikov, E. Y.; Muradov, M. B.; Akperov, O. H.; Eyvazova, G. M.; Puskás, R.; Madarász, D.; Nagy, L.; Kukovecz, Á; Kónya, Z. Synthesis and characterization of polyvinyl alcohol based multiwalled carbon nanotube nanocomposites. *Physica E: Low-dimensional Systems and Nanostructures.* **2014**, *61*, 129−34.

(39) Sundararajan, S.; Samui, A. B.; Kulkarni, P. S. Synthesis and characterization of poly (ethylene glycol)(PEG) based hyperbranched polyurethanes as thermal energy storage materials. *Thermochim. Acta* **2017**, *650*, 114−22.

(40) Kulasekaran, P.; Mahimai, B. M.; Deivanayagam, P. Novel cross-linked poly (vinyl alcohol)-based electrolyte membranes for fuel cell applications. *RSC advances.* **2020**, *10*, 26521−7.

(41) Kumar, A.; Kumar, N.; Sharma, Y.; Leu, J.; Tseng, T. Y. Synthesis of free-standing flexible rGO/MWCNT films for symmetric super-capacitor application. *Nanoscale research letters.* **2019**, *14*, 1−7.

(42) Díez-Pascual, A. M. Nanoparticle reinforced polymers. *Polymers.* **2019**, *11*, 625.

(43) Das, A.; Thakur, A. K. Effect on ion dissociation in MWCNT-based polymer nanocomposite. *Ionics.* **2017**, *23*, 2845−53.

(44) Salam, M. A.; Burk, R. Synthesis and characterization of multi-walled carbon nanotubes modified with octadecylamine and poly-ethylene glycol. *Arabian Journal of Chemistry.* **2017**, *10*, 5921−7.

(45) Raju, C. H.; Rao, J. L.; Reddy, B. C.; Veera Brahham, K. Thermal and IR studies on copper doped polyvinyl alcohol. *Bulletin of Materials Science* **2007**, *30* (3), 215−8.

(46) Lobo, B.; Veena, G. Experimental investigations on nano-titania incorporated polyvinyl alcohol-polyvinyl pyrrolidone composite films. *Polymer-Plastics Technology and Materials* **2021**, *60*, 1697−717 Oct 13.

(47) Hema, M.; Selvasekerapandian, S.; Sakunthala, A.; Arunkumar, D.; Nithya, H. Structural, vibrational and electrical characterization of PVA-NH4Br polymer electrolyte system. *Physica B: Condensed Matter.* **2008**, *403*, 2740−7.

(48) Hema, M.; Selvasekarapandian, S.; Arunkumar, D.; Sakunthala, A.; Nithya, H. F. FTIR, XRD and ac impedance spectroscopic study on PVA based polymer electrolyte doped with NH4X (X= Cl, Br, I). *Journal of Non-Crystalline Solids.* **2009**, *355*, 84−90.

(49) Reddy Polu, A.; Kumar, R. Impedance spectroscopy and FTIR studies of PEG-based polymer electrolytes. *E-Journal of Chemistry.* **2011**, *8*, 347−53.

(50) Mallaiah, Y.; Jeedi, V. R.; Swarnalatha, R.; Raju, A.; Reddy, S. N.; Chary, A. S. Impact of polymer blending on ionic conduction mechanism and dielectric properties of sodium-based PEO-PVdF solid polymer electrolyte systems. *J. Phys. Chem. Solids* **2021**, *155*, 110096.

(51) Sadiq, M.; Raza, M. M.; Chaurasia, S. K.; Zulfequar, M.; Ali, J. Studies on flexible and highly stretchable sodium ion conducting blend polymer electrolytes with enhanced structural, thermal, optical, and electrochemical properties. *Journal of Materials Science: Materials in Electronics.* **2021**, *32*, 19390−411.

(52) Ramamohan, K.; Achari, V. B.; Sharma, A. K.; Xiuyang, L. Electrical and structural characterization of PVA/PEG polymer blend electrolyte films doped with NaClO4. *Ionics.* **2015**, *21*, 1333−40.

(53) Rajavardhana Rao, T.; Omkaram, I.; Sumalatha, B.; Veera Brahham, K.; Linga Raju, C. Electron paramagnetic resonance and

optical absorption studies of manganese ions doped in polyvinyl (alcohol) complexed with polyethylene glycol polymer films. *Ionics.* **2012**, *18*, 695−701.

(54) Mansur, H. S.; Sadahira, C. M.; Souza, A. N.; Mansur, A. A. FTIR spectroscopy characterization of poly (vinyl alcohol) hydrogel with different hydrolysis degree and chemically crosslinked with gluta-raldehyde. *Materials Science and Engineering: C* **2008**, *28*, 539−48.

(55) Duraikkan, V.; Sultan, A. B.; Nallaperumal, N.; Shunmuganarayanan, A. Structural, thermal and electrical properties of polyvinyl alcohol/poly (vinyl pyrrolidone)-sodium nitrate solid polymer blend electrolyte. *Ionics.* **2018**, *24*, 139−51.

(56) Pritam; Arya, A.; Sharma, A. L. Dielectric relaxations and transport properties parameter analysis of novel blended solid polymer electrolyte for sodium-ion rechargeable batteries. *J. Mater. Sci.* **2019**, *54*, 7131−55.

(57) Dibbern-Brunelli, D.; Atvars, T. D.; Joekes, I.; Barbosa, V. C. Mapping phases of poly (vinyl alcohol) and poly (vinyl acetate) blends by FTIR microspectroscopy and optical fluorescence microscopy. *J. Appl. Polym. Sci.* **1998**, *69*, 645−55.

(58) Goumri, M.; Venturini, J. W.; Bakour, A.; Khenfouch, M.; Baitoul, M. Tuning the luminescence and optical properties of graphene oxide and reduced graphene oxide functionalized with PVA. *Appl. Phys. A: Mater. Sci. Process.* **2016**, *122*, 1−8.

(59) Jyoti, J.; Arya, A. K.; Chockalingam, S.; Yadav, S. K.; Subhedar, K. M.; Dhakate, S. R.; Singh, B. P. Mechanical, electrical and thermal properties of graphene oxide-carbon nanotube/ABS hybrid polymer nanocomposites. *Journal of Polymer Research.* **2020**, *27*, 1−6.

(60) Yanmaz, E.; Doğan, M.; Turhan, Y. Effect of sodium dodecyl sulfate on thermal properties of polyvinyl alcohol (PVA)/modified single-walled carbon nanotube (SWCNT) nanocomposites. *Diamond Relat. Mater.* **2021**, *115*, 108359.

(61) Brubaker, Z. E.; Langford, J. J.; Kapsimalis, R. J.; Niedziela, J. L. Quantitative analysis of Raman spectral parameters for carbon fibers: practical considerations and connection to mechanical properties. *J. Mater. Sci.* **2021**, *56* (27), 15087−121.

(62) Barzegar, F.; Bello, A.; Fabiane, M.; Khamlich, S.; Momodu, D.; Taghizadeh, F.; Dangbegnon, J.; Manyala, N. Preparation and characterization of poly (vinyl alcohol)/graphene nanofibers synthe-sized by electrospinning. *Journal of Physics and Chemistry of Solids.* **2015**, *77*, 139−45.

(63) Ben, J.; Song, Z.; Liu, X.; Lü, W.; Li, X. Fabrication and electrochemical performance of PVA/CNT/PANI flexible films as electrodes for supercapacitors. *Nanoscale Research Letters.* **2020**, *15*, 1−8.

(64) Maitra, T.; Sharma, S.; Srivastava, A.; Cho, Y. K.; Madou, M.; Sharma, A. Improved graphitization and electrical conductivity of suspended carbon nanofibers derived from carbon nanotube/polyacrylonitrile composites by directed electrospinning. *Carbon.* **2012**, *50*, 1753−61.

(65) Ahn, J. H.; Kim, Y. J.; Wang, G. X. Electrochemical properties of carbon nanotube-dispersed PEO-LiX electrolytes. *Metals and materials international.* **2006**, *12*, 69−73.

(66) Kovacs, J. Z.; Andresen, K.; Pauls, J. R.; Garcia, C. P.; Schossig, M.; Schulte, K.; Bauhofer, W. Analyzing the quality of carbon nanotube dispersions in polymers using scanning electron microscopy. *Carbon* **2007**, *45*, 1279−88.

(67) Nurly, H.; Yan, Q.; Song, B.; Shi, Y. Effect of carbon nanotubes reinforcement on the polyvinyl alcohol-polyethylene glycol double-network hydrogel composites: a general approach to shape memory and printability. *Eur. Polym. J.* **2019**, *110*, 114−22.

(68) Lai, D.; Wei, Y.; Zou, L.; Xu, Y.; Lu, H. Wet spinning of PVA composite fibers with a large fraction of multi-walled carbon nanotubes. *Progress in Natural Science: Materials International.* **2015**, *25*, 445−52.

(69) Chen, W.; Tao, X.; Xue, P.; Cheng, X. Enhanced mechanical properties and morphological characterizations of poly (vinyl alcohol)-carbon nanotube composite films. *Appl. Surf. Sci.* **2005**, *252*, 1404−9.

(70) Wang, S.; Liu, Y.; Huang, S.; Wu, H.; Li, Y.; Tian, Z.; Jiang, Z. Pebax-PEG-MWCNT hybrid membranes with enhanced CO$_2$ capture properties. *J. Membr. Sci.* **2014**, *460*, 62−70.

(71) Choi, C. S.; Park, B. J.; Choi, H. J. Electrical and rheological characteristics of poly (vinyl acetate)/multi-walled carbon nanotube nanocomposites. *Diamond and related materials.* **2007**, *16*, 1170−3.

(72) Devangamath, S. S.; Lobo, B.; Masti, S. P.; Narasagoudr, S. Thermal, mechanical, and AC electrical studies of PVA-PEG-Ag$_2$S polymer hybrid material. *Journal of Materials Science: Materials in Electronics.* **2020**, *31*, 2904−17.

(73) Sharma, B.; Sandilya, A.; Sharma, S.; Garg, M.; Sadhu, S. D. Thermo-mechanical investigation of PEG-PVA biohybrid active film grafted with copper nanoparticles for packaging applications. *Bulletin of Materials Science.* **2021**, *44*, 1−1.

(74) Heiba, Z. K.; Mohamed, M. B.; Ahmed, S. I. Exploring the physical properties of PVA/PEG polymeric material upon doping with nano gadolinium oxide. *Alexandria Engineering Journal.* **2022**, *61*, 3375−83.

(75) Hirankumar, G.; Mehta, N. Effect of incorporation of different plasticizers on structural and ion transport properties of PVA-LiClO$_4$ based electrolytes. *Heliyon.* **2018**, *4*, 00992.

(76) Li, Z.; He, W.; Xu, J.; Jiang, M. Preparation and characterization of in situ grafted/crosslinked polyethylene glycol/polyvinyl alcohol composite thermal regulating fiber. *Solar Energy Materials and Solar Cells.* **2015**, *140*, 193−201.

(77) Shao, L.; Li, J.; Guang, Y.; Zhang, Y.; Zhang, H.; Che, X.; Wang, Y. PVA/polyethyleneimine-functionalized graphene composites with optimized properties. *Materials & Design.* **2016**, *99*, 235−42.

(78) Ostrander, J. W.; Wang, L.; Ali Kizi, T.; Dajani, J. A.; Carr, A. V.; Teeters, D.; Lamar, A. A. Enhanced Conductivity via Extraction of Hydrocarbon Templates from Nanophase-Separated PEO-LiOTf Polymer Electrolyte Films. *ACS omega.* **2020**, *5*, 20567−74.

(79) Pundir, S. S.; Mishra, K.; Rai, D. K. Structural, thermal and electrochemical studies of PVA/PVP—NH$_4$SCN—[C2C1Im][SCN] polymer electrolyte system. *Journal of Materials Science: Materials in Electronics.* **2021**, *32*, 1476−90.

(80) Kim, M. J.; Lee, J.; Jung, D.; Shim, S. E. Electrospun poly (vinyl alcohol) nanofibers incorporating PEGylated multi-wall carbon nanotube. *Synthetic metals.* **2010**, *160*, 1410−4.

(81) Ates, M.; Karazehir, T.; Arican, F.; Eren, N. Electrolyte type and concentration effects on poly (3-(2-aminoethyl thiophene) electro-coated on glassy carbon electrode via impedimetric study. *Iranian Polymer Journal.* **2013**, *22*, 199−208.

(82) Polu, A. R.; Kumar, R. AC impedance and dielectric spectroscopic studies of Mg^{2+} ion conducting PVA-PEG blended polymer electrolytes. *Bulletin of Materials Science.* **2011**, *34*, 1063−7.

(83) Yu, C. R.; Wu, D. M.; Liu, Y.; Qiao, H.; Yu, Z. Z.; Dasari, A.; Du, X. S.; Mai, Y. W. Electrical and dielectric properties of polypropylene nanocomposites based on carbon nanotubes and barium titanate nanoparticles. *Compos. Sci. Technol.* **2011**, *71*, 1706−12.

(84) Rag, S. A.; Dhamodharan, D.; Selvakumar, M.; Bhat, S.; De, S.; Byun, H. S. Impedance spectroscopic study of biodegradable PVA/PVP doped TBAI ionic liquid polymer electrolyte. *Journal of Industrial and Engineering Chemistry* **2022**, *111*, 43.

(85) Abdullah, O. G.; Ahmed, H. T.; Tahir, D. A.; Jamal, G. M.; Mohamad, A. H. Influence of PEG plasticizer content on the proton-conducting PEO: MC-NH4I blend polymer electrolytes based films. *Results in Physics.* **2021**, *23*, 104073.

(86) Shubha, A.; Manohara, S. R.; Siddlingeshwar, B.; Daima, H. K.; Singh, M.; Revaprasadu, N. Ternary poly (2-ethyl-2-oxazoline)-polyvinylpyrrolidone-graphene nanocomposites: thermal, electrical, dielectric, mechanical, and antibacterial profiling. *Diamond Relat. Mater.* **2022**, *125*, 109001.

(87) Saxena, H.; Bhattacharya, B.; Jadhav, N. A.; Singh, V. K.; Shukla, S.; Dubey, M.; Singh, P. K. Multiwall carbon-nanotube-doped ion conducting polymer electrolyte for electrochemical application. *Journal of Experimental Nanoscience.* **2014**, *9*, 444−51.

(88) Ibrahim, S.; Yasin, S. M.; Ng, M. N.; Ahmad, R.; Johan, M. R. Impedance spectroscopy of carbon nanotube/solid polymer electrolyte composites. *Solid state communications.* **2011**, *151*, 1828−32.

(89) Fan, L.; Yu, L.; Xu, F.; Qin, G.; Chen, Q. Preparation of PVA-based composite alkaline solid polymer electrolyte with La_2O_3 nanoparticle filler. *Journal of Nanoparticle Research.* 2021, 23, 1−9.

(90) Amiri, H.; Mohsennia, M. Impedance study of PVA/PEG/$LiClO_4$/TiO_2 nanocomposite solid polymer blend electrolyte. *Journal of Materials Science: Materials in Electronics.* 2017, 28, 4586−92.

(91) Abdelrazek, E. M.; Abdelghany, A. M.; Tarabiah, A. E.; Zidan, H. M. AC conductivity and dielectric characteristics of PVA/PVP nanocomposite filled with MWCNTs. *Journal of Materials Science: Materials in Electronics.* 2019, 30, 15521−33.

(92) Cholant, C. M.; Rodrigues, M. P.; Balboni, R. D.; Krüger, L. U.; Lemos, R. M.; Lopes, D. F.; Pawlicka, A.; Avellaneda, C. O. Study of the effect of $LiClO_4$ concentration on the ionic transport of solid polymer electrolyte based on poly (vinyl alcohol)/gum Arabic. *Ionics* 2022, 1−5.

(93) Ibrahim, S.; Yasin, S. M.; Nee, N. M.; Ahmad, R.; Johan, M. R. Conductivity and dielectric behaviour of PEO-based solid nano-composite polymer electrolytes. *Solid state communications.* 2012, 152, 426−34.

(94) Sadiq, M.; Raza, M. M.; Zulfequar, M.; Ali, J. Facile synthesis of highly flexible sodium ion conducting polyvinyl alcohol (PVA)-polyethylene glycol (PEG) blend incorporating reduced graphene-oxide (rGO) composites for electrochemical devices application. *Journal of Polymer Research.* 2022, 29, 1−23.

(95) Alam, R. B.; Ahmad, M. H.; Islam, M. R. Effect of MWCNT nanofiller on the dielectric performance of bio-inspired gelatin-based nanocomposites. *RSC Advances.* 2022, 12, 14686−97.

(96) Kumar, D.; Gohel, K.; Kanchan, D. K.; Mishra, K. Dielectrics and battery studies on flexible nanocomposite gel polymer electrolyte membranes for sodium batteries. *Journal of Materials Science: Materials in Electronics.* 2020, 31, 13249−60.

(97) Laxmayyaguddi, Y.; Mydur, N.; Shankar Pawar, A.; Hebri, V.; Vandana, M.; Sanjeev, G.; Hundekal, D. Modified thermal, dielectric, and electrical conductivity of PVDF-HFP/$LiClO_4$ polymer electrolyte films by 8 MeV electron beam irradiation. *ACS omega.* 2018, 3, 14188−200.

(98) Arya, A.; Sadiq, M.; Sharma, A. L. Effect of variation of different nanofillers on structural, electrical, dielectric, and transport properties of blend polymer nanocomposites. *Ionics.* 2018, 24, 2295−319.

(99) Johari, N. S.; Adnan, S. B.; Mohamed, N. S.; Ahmad, N. Structural and electrical properties of Na_2ZnSiO_4-Py14TFSI hybrid solid electrolyte. *Ceram. Int.* 2020, 46, 8039−46.

(100) Prajapati, G. K.; Gupta, P. N. Comparative study of the electrical and dielectric properties of PVA-PEG-Al_2O_3-MI (M= Na, K, Ag) complex polymer electrolytes. *Physica B: Condensed Matter.* 2011, 406, 3108−13.

(101) Vanitha, D.; Bahadur, S. A.; Nallamuthu, N.; Athimoolam, S.; Manikandan, A. Electrical impedance studies on sodium ion conducting composite blend polymer electrolyte. *Journal of Inorganic and Organometallic Polymers and Materials.* 2017, 27, 257−65.

(102) Nangia, R.; Shukla, N. K.; Sharma, A. Frequency and temperature-dependent impedance spectroscopy of PVA/PEG polymer blend film. *High Performance Polymers.* 2018, 30, 918−26.

(103) Arya, A.; Sharma, A. L. Structural, electrical properties and dielectric relaxations in Na+-ion-conducting solid polymer electrolyte. *Journal of Physics: Condensed Matter.* 2018, 30, 165402.

(104) Radha, K. P.; Selvasekarapandian, S.; Karthikeyan, S.; Hema, M.; Sanjeeviraja, C. Synthesis and impedance analysis of proton-conducting polymer electrolyte PVA: NH4F. *Ionics.* 2013, 19, 1437−47.

(105) Arya, A.; Sharma, A. L. Tailoring of the structural, morphological, electrochemical, and dielectric properties of solid polymer electrolyte. *Ionics.* 2019, 25, 1617−32.

(106) Kumar, S.; Prajapati, G. K.; Saroj, A. L.; Gupta, P. N. Structural, electrical and dielectric studies of nano-composite polymer blend electrolyte films based on (70-x) PVA-x PVP-NaI-SiO_2. *Physica B: Condensed Matter.* 2019, 554, 158−64.

(107) Arya, A.; Sharma, A. L. Effect of salt concentration on dielectric properties of Li-ion conducting blend polymer electrolytes. *Journal of Materials Science: Materials in Electronics.* 2018, 29, 17903−20.

(108) Sadiq, M.; Raza, M. M.; Murtaza, T.; Zulfequar, M.; Ali, J. Sodium ion-conducting polyvinylpyrrolidone (PVP)/Polyvinyl alcohol (PVA) blend electrolyte films. *J. Electron. Mater.* 2021, 50, 403−18.

(109) Singh, P.; Bharati, D. C.; Kumar, H.; Saroj, A. L. Ion transport mechanism and dielectric relaxation behavior of PVA-imidazolium ionic liquid-based polymer electrolytes. *Phys. Scr.* 2019, 94, 105801.

(110) Arya, A.; Sharma, A. L. Temperature and salt-dependent dielectric properties of blend solid polymer electrolyte complexed with LiBOB. *Macromolecular Research.* 2019, 27, 334−45.

(111) Hei, Z.; Wu, S.; Zheng, H.; Liu, H.; Duan, H. Increasing the electrochemical stability window for polyethylene-oxide-based solid polymer electrolytes by understanding the affecting factors. *Solid State Ionics.* 2022, 375, 115837.

(112) Yang, J.; Zhang, H.; Zhou, Q.; Qu, H.; Dong, T.; Zhang, M.; Tang, B.; Zhang, J.; Cui, G. Safety-enhanced polymer electrolytes for sodium batteries: recent progress and perspectives. *ACS applied materials & interfaces.* 2019, 11, 17109−27.

(113) Anilkumar, K. M.; Jinisha, B.; Manoj, M.; Jayalekshmi, S. Poly (ethylene oxide)(PEO)-Poly (vinyl pyrrolidone)(PVP) blend polymer based solid electrolyte membranes for developing solid state magnesium ion cells. *Eur. Polym. J.* 2017, 89, 249−62.

(114) Aziz, S. B.; Dannoun, E.; Hamsan, M. H.; Abdulwahid, R. T.; Mishra, K.; Nofal, M. M.; Kadir, M. F. Improving EDLC device performance constructed from plasticized magnesium ion conducting chitosan-based polymer electrolytes via metal complex dispersion. *Membranes.* 2021, 11, 289.

(115) Kumar, D.; Hashmi, S. A. Ion transport and ion-filler-polymer interaction in poly (methyl methacrylate)-based, sodium ion conducting, gel polymer electrolytes dispersed with silica nanoparticles. *Journal of Power Sources.* 2010, 195, 5101−8.

(116) Evans, J.; Vincent, C. A.; Bruce, P. G. Electrochemical measurement of transference numbers in polymer electrolytes. *Polymer.* 1987, 28, 2324−8.